ORIGINAL ARTICLE

A Functional Anatomic Defect of the Cystic Fibrosis Airway

Susan E. Birket[1]*, Kengyeh K. Chu[2,3,4]*, Linbo Liu[2,3], Grace H. Houser[5], Bradford J. Diephuis[2,4,6], Eric J. Wilsterman[2,3], Gregory Dierksen[2,3], Marina Mazur[7], Suresh Shastry[1,7], Yao Li[1,7], John D. Watson[1], Alexander T. Smith[1], Benjamin S. Schuster[8,9], Justin Hanes[8,10,11,12], William E. Grizzle[13], Eric J. Sorscher[1,7,14], Guillermo J. Tearney[2,4,6,15]‡, Steven M. Rowe[1,5,7,14]‡

[1]Department of Medicine, [5]Department of Pediatrics, [7]Cystic Fibrosis Research Center, [13]Department of Pathology, and [14]Department of Cellular, Developmental, and Integrative Biology, University of Alabama at Birmingham, Birmingham, Alabama; [2]Wellman Center for Photomedicine, [3]Department of Dermatology, and [15]Department of Pathology, Massachusetts General Hospital, Boston, Massachusetts; [4]Harvard Medical School, Boston, Massachusetts; [6]Harvard-MIT Division of Health Sciences and Technology, Cambridge, Massachusetts; [8]Department of Biomedical Engineering, [9]Center for Nanomedicine, [10]Department of Ophthalmology, and [11]Department of Neurosurgery, Johns Hopkins Hospital, Baltimore, Maryland; and [12]Institute for NanoBioTechnology and the Center for Cancer Nanotechnology Excellence, Baltimore, Maryland

Abstract

Rationale: The mechanisms underlying cystic fibrosis (CF) lung disease pathogenesis are unknown.

Objectives: To establish mechanisms linking anion transport with the functional microanatomy, we evaluated normal and CF piglet trachea as well as adult swine trachea in the presence of selective anion inhibitors.

Methods: We investigated airway functional microanatomy using microoptical coherence tomography, a new imaging modality that concurrently quantifies multiple functional parameters of airway epithelium in a colocalized fashion.

Measurements and Main Results: Tracheal explants from wild-type swine demonstrated a direct link between periciliary liquid (PCL) hydration and mucociliary transport (MCT) rates, a relationship frequently invoked but never experimentally confirmed. However, in CF airways this relationship was completely disrupted, with greater PCL depths associated with slowest transport rates. This disrupted relationship was recapitulated by selectively inhibiting bicarbonate transport *in vitro* and *ex vivo*. CF mucus exhibited increased viscosity *in situ* due to the absence of bicarbonate transport, explaining defective MCT that occurs even in the presence of adequate PCL hydration.

Conclusions: An inherent defect in CF airway surface liquid contributes to delayed MCT beyond that caused by airway dehydration alone and identifies a fundamental mechanism underlying the pathogenesis of CF lung disease in the absence of antecedent infection or inflammation.

Keywords: cystic fibrosis; airway epithelium; optical coherence tomography; mucus transport; viscosity

(Received in original form April 13, 2014; accepted in final form June 23, 2014)

*First authors contributed equally to this manuscript.

‡Shared equal responsibility as principal investigators.

Supported by the National Heart, Lung, and Blood Institute grants P01HL51811 (J.H.), R01HL116213 (G.J.T. and S.M.R.), and 5T32HL105346-04 (S.E.B.) and the National Institute of Diabetes and Digestive and Kidney Diseases grant P30DK072482 (E.J.S.) and the National Institute of Bioimaging and Bioengineering grant R01EB003558 (J.H.) of the National Institutes of Health, the Research Development Program (R464-CF), and the Mucociliary Clearance Consortium (J.H., G.J.T., and S.M.R.) of the Cystic Fibrosis Foundation, the Flatley Foundation (K.K.C., G.D., G.J.T., and S.M.R.), and the Dixon Foundation (G.H.H.).

Author Contributions: L.L., S.E.B., E.J.S., G.J.T., and S.M.R. conceived of the experiments; L.L., G.H.H., S.E.B., K.K.C., B.J.D., G.D., M.M., S.S., Y.L., J.D.W., A.T.S., and S.M.R. performed research; L.L., G.H.H., S.E.B., K.K.C., B.J.D., E.J.W., G.D., S.S., Y.L., J.D.W., B.S.S., J.H., W.E.G., E.J.S., G.J.T., and S.M.R. analyzed the data; W.E.G., E.J.S., B.S.S., J.H., G.J.T., and S.M.R. contributed reagents, materials, and/or analysis tools; L.L., S.E.B., G.H.H., K.K.C., E.J.S., G.J.T., and S.M.R. wrote the manuscript; and G.J.T. and S.M.R. supervised the project.

Correspondence and requests for reprints should be addressed to Steven M. Rowe, M.D., M.S.P.H., MCLM 706, 1720 2nd Avenue South, Birmingham, AL 35294-0006. E-mail: smrowe@uab.edu; or Guillermo J. Tearney, M.D., Ph.D., 55 Fruit Street, BHX604A, Boston, MA 02114. E-mail: gtearney@partners.org

This article has an online supplement, which is accessible from this issue's table of contents at www.atsjournals.org

This article has embedded videos, which play in place from both the online PDF or HTML versions. If you cannot view Flash videos on your device, please access the original uncompressed videos at http://www.atsjournals.org/doi/suppl/10.1164/rccm.201404-0670OC. To play, mouse over the image and click on the arrow that will appear in the center or on the lower left.

Am J Respir Crit Care Med Vol 190, Iss 4, pp 421–432, Aug 15, 2014

Originally Published in Press as DOI: 10.1164/rccm.201404-0670OC on July 16, 2014
Internet address: www.atsjournals.org

At a Glance Commentary

Scientific Knowledge on the Subject: The mechanisms underlying cystic fibrosis (CF) airway pathophysiology are unknown and remain a topic of debate. Current hypotheses include depleted airway surface liquid and altered mucus biosynthesis secondary to absent CF transmembrane conductance regulator (CFTR)-mediate bicarbonate transport.

What This Study Adds to the Field: Using innovative technology enabling concurrent quantification of multiple functional parameters of airway epithelium in a colocalized fashion, we have shown that the interrelationship between airway hydration and mucus transport is altered in CF. This disruption appears to be mediated by absence of bicarbonate transport and may constitute a fundamental mechanism underlying the pathogenesis of CF lung disease.

Cystic fibrosis (CF) causes significant morbidity and mortality from progressive lung disease (1). The primary defect in CF is dysfunction of the CF transmembrane conductance regulator (CFTR), an epithelial transporter of chloride and bicarbonate (2–4). In the lungs, deficient CFTR-mediated anion transport is believed to cause delayed mucociliary clearance (MCC), although the underlying mechanism remains a topic of importance and debate. A longstanding hypothesis suggests that deficient chloride transport combined with sodium absorption across the airway epithelia depletes the airway surface liquid (ASL), including the periciliary liquid (PCL) and the overlying mucus (5–7). This hypothesis has been supported by evidence in CF primary human bronchial epithelial (HBE) cell culture models and excised tissues (5, 6, 8, 9). The CFTR defect also reduces mucus secretion in CF airway glands (10–12), possibly contributing to inadequate ASL hydration and decreased MCC.

This hypothesis has been subject to renewed controversy since the development of a swine model that recapitulates many features of CF lung disease (13, 14) but does not exhibit sodium hyperabsorption or PCL depletion (15). Alternative mechanisms for CF pathogenesis have been proposed, including the suggestion that reduced airway pH (16, 17) or abnormal mucus biosynthesis (18–21) may be major contributors. Quinton has hypothesized that the absence of CFTR-mediated bicarbonate transport may cause abnormal CF mucus in the lungs, renewing interest in the term "mucoviscidosis" (21). Although bicarbonate secretion in the airway has been shown (22), its impact on mucus adhesion has so far been limited to studies of murine intestine (18, 19). Others have suggested that CF mucus is not inherently abnormal but is altered by secondary phenomena such as inflammation and gland hyperplasia (23).

To address these critical questions, airway parameters must be evaluated concurrently *in situ* rather than using asynchronous measures or fixed tissues. Recently, we have developed microoptical coherence tomography (μOCT), which enables real-time, noninvasive imaging of the epithelial surface of living airways, at submicron resolution (24–26). μOCT images are acquired without use of contrast dyes, exogenous microparticles, tissue fixation, or other manipulations that limit current airway assessment techniques. Accuracy for simultaneously measuring microanatomic parameters relevant to the airway has been validated (24).

In the present study, we investigated the functional airway microanatomy of the CF lung using μOCT and state-of-the-art models, including primary HBE cells and fresh CFTR (−/−) porcine tissues. Our findings establish that increased ASL viscosity is a fundamental aspect of the CF airway defect, even in the absence of infection and inflammation, providing a mechanism of mucoviscidosis operative in multiple organs affected by CF.

Methods

Detailed methods are provided in the online supplement.

Study Approvals

Procedures involving human cells and tissue were approved by institutional review boards at the University of Alabama Birmingham (IRB numbers X080625002, X110916018, and X101111014) and Massachusetts General Hospital (IRB number 2008P000178). Animal use was approved by the University of Alabama Birmingham Institutional Animal Care and Use Committee.

Primary HBE Cell Cultures

Primary HBE cells were derived from lung explants as previously described (27–29). Collected epithelial cells were grown in differentiating media for at least 6 to 8 weeks until terminally differentiated. Cells were apically washed with PBS 48 hours before the experiment. In some experiments, cells were cultured in media depleted of bicarbonate, with and without acetazolamide (100 μM).

Swine Tissue Culture

CFTR (+/+) and CFTR (−/−) piglet tracheas were obtained from Exemplar Genetics. We used a modified tissue handling and preparation protocol based on the methods of Ballard and colleagues (30). For *ex vivo* analysis, tracheae were equilibrated to steady state at physiologic conditions for at least 4 hours in an environmentally controlled chamber then subsequently imaged by μOCT.

Shear Stress

In some experiments, shear stress was applied using a rocker from Boekel Scientific set to 20 rotations per minute to mimic swine respiratory rate. The peak amplitude of applied shear stress was 0.114 dynes/cm^2 at the luminal surface.

Bicarbonate Inhibition

Normal Yorkshire pigs were obtained from Auburn University at age 3 to 4 months. Tracheae were treated with dimethyl sulfoxide vehicle control, 4,4'-dinitrostilbene-2,2'-disulphonic acid (DNDS, 3 mM), or bumetanide (100 μM) and were incubated and imaged, as above. Acetylcholine (100 μM) was subsequently added to produce mucus for collection.

Image Acquisition

Measurements of functional microanatomic parameters in cultured cells and tissue were performed using microoptical coherence tomography (μOCT) (24).

Image Analysis

Quantitative analysis of images provided ASL and PCL depths and ciliary beat frequency (CBF) and MCT rate. For each

HBE monolayer, images were acquired 1 mm from the filter edge. For trachea, images were acquired at randomly chosen locations on the mucosal surface. For regional analyses, when mucus was absent, colocalized comparison was not performed because MCT could not be accurately measured in the absence of visible mucus.

Histology

Sections of swine trachea were fixed in 10% neutral buffered formalin and embedded in paraffin. Sections were stained with hematoxylin and eosin.

Fluorescence Recovery after Photobleaching

To measure fluorescence recovery after photobleaching (FRAP) in HBE cells or trachea explants, ASL was stained with fluorescein isothiocyanate (10 μl at 1 mg/ml in PBS) and incubated for 30 minutes at 37°C (20). A circular area of approximately 3- to 5-μm diameter on the ASL surface was bleached with a 5-mW argon laser and 30-mW diode laser, and then fluorescence intensity was quantified as fluorescein isothiocyanate labeled ASL filled the bleached area. Images were acquired by confocal microscopy (sequential XY scans) until maximal recovery was reached. The recovery curves of normalized values were plotted using one phase association equation. Additional detail is provided online.

Particle Tracking Microrheology

Particle-tracking microrheological techniques were used to measure viscosity of mucus on non-CF and CF HBE cell cultures and from mucus collected from pig tracheae (31, 32). Fluorescent PEG-PS beads (2.0×10^{11} particles/ml) were added to apical surface of cells or mucus placed in 1 cm on glass slides. Samples were incubated at room temperature to allow distribution of particles. Fluorescence time-series images were acquired using an inverted microscope at a frame rate of approximately 17 frames per second. Resulting particle tracks were analyzed with custom MATLAB procedures.

Statistics

Statistical analysis was performed in GraphPad Prism version 6.0. Statistics are presented as mean ± SEM, except as indicated. Statistical methods are discussed in the online supplement.

Results

Altered Functional Microanatomy of CF-derived (HBE) Cells

μOCT imaging provides an accurate and precise measure of the length of fully extended cilia, and thus the PCL layer, and is colocalized with other parameters of the epithelial surface (*see* Figure E1 in the online supplement) (24). With this advantage in mind, we evaluated cultured primary HBE cell monolayers under physiologic conditions to determine differences in the functional microanatomy. Representative

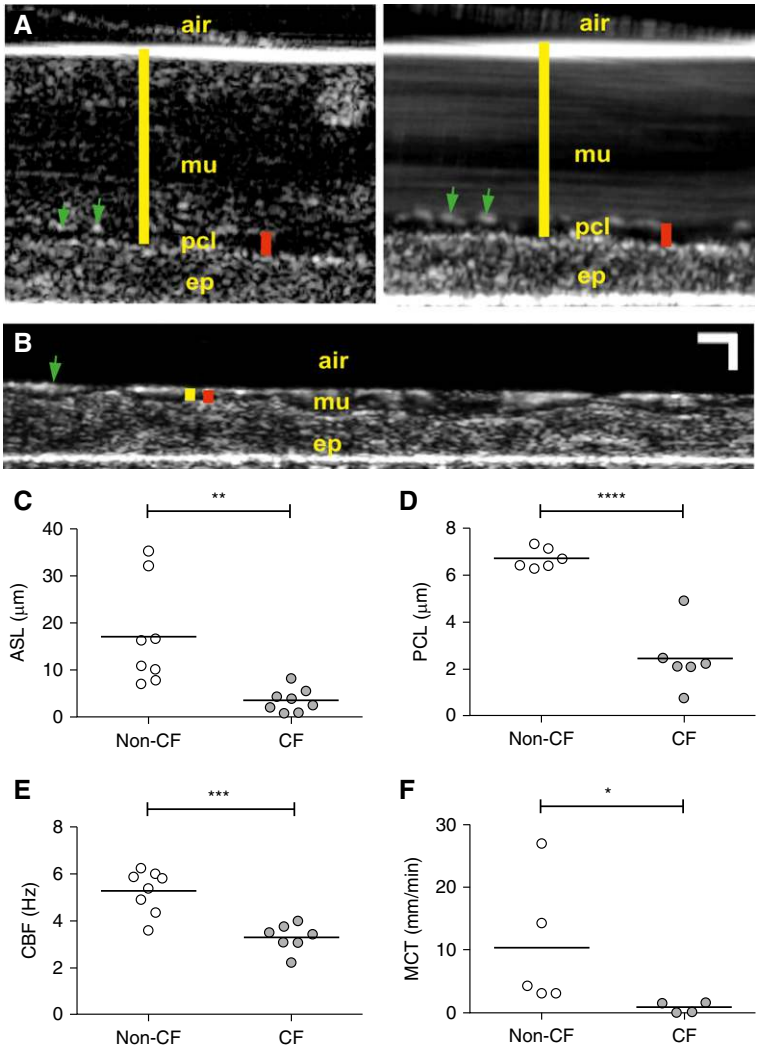

Figure 1. Microoptical coherence tomography (μOCT) imaging of human bronchial epithelial (HBE) respiratory epithelia. (*A*) μOCT images of non–cystic fibrosis (CF) HBE cells grown in culture. Cilia tips (*green arrows*), mucus layer (mu), airway surface liquid (ASL) layer (*yellow bar*), and periciliary liquid (PCL) layer (*red bar*) are seen. PCL and cilia tips are more readily discerned in time-averaged image over 10 s (*right*) as compared with static image (*left*). ASL depth (*yellow bar*) is defined by the distance between the air–mucus interface and the surface of the epithelial layer (ep). PCL depth (*red bar*) is defined by the distance between the mucus layer and the epithelial surface. (*B*) Depleted ASL (*yellow bar*) and PCL (*red bar*) with cilia (*green arrow*) entangled within the mucus are visible in a μOCT image of HBE cells derived from a subject with CF. Horizontal and vertical scale bars: 10 μm. *See* also Video 1. (*C–F*) Analysis of μOCT images from HBE cells derived from non-CF and CF donors and grown in culture yields numerical values for functional and anatomic parameters. ASL depth (*C*), PCL depth (*D*), ciliary beat frequency (CBF; *E*), and mucociliary transport (MCT) rate (*F*) are shown. $^{*}P < 0.05$, $^{**}P < 0.005$, $^{***}P < 0.0005$, $^{****}P < 0.00005$. Each symbol represents mean value from independent HBE monolayer; at least four donors were evaluated per condition. Note: a component of non-CF control data was previously reported (24, 35).

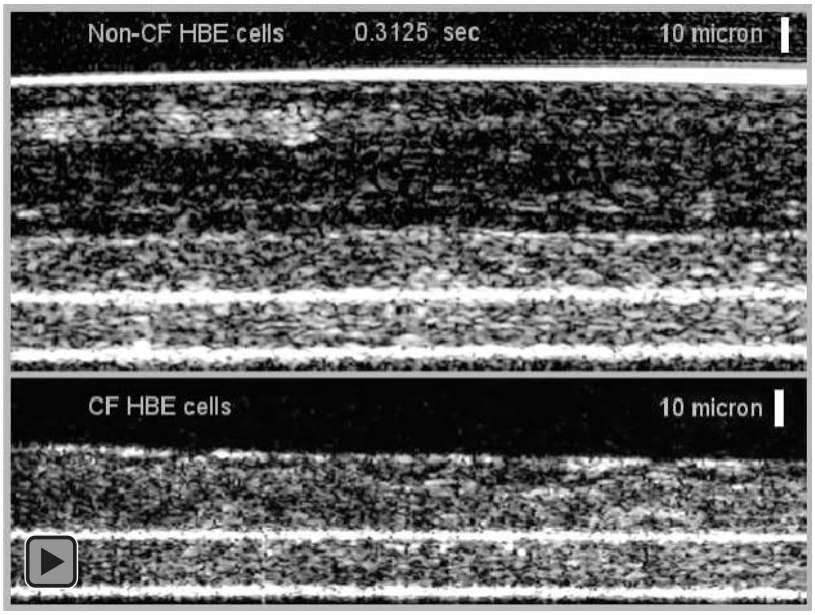

Video 1. Microoptical coherence tomography (μOCT) video showing well-differentiated primary human bronchial epithelial (HBE) cultures derived from a subject without cystic fibrosis (CF) (*top*) and a subject with CF (*bottom*).

two-dimensional images are shown in Figures 1A and 1B, and Video 1. Although regionally heterogeneous across the epithelial surface, CF monolayers exhibited ASL and PCL depletion compared with non-CF HBE. Cilia in the CF monolayer were entangled within the mucus, in contrast to those in the wild-type (WT) HBE monolayer in which cilia tips can be clearly seen upright within the PCL and at an angle to the epithelial surface. Functional parameters derived from μOCT imaging provided simultaneous measurements of ASL, PCL, CBF, and MCT across multiple donors and various regions of interest (Figures 1C–1F). The ASL depth of CF HBE cells was significantly lower than non-CF HBE cells (3.5 ± 0.9 μm CF vs. 17.0 ± 3.9 μm non-CF, $P < 0.005$); the decrement in PCL depth was also pronounced (2.4 ± 0.6 μm CF vs. 6.7 ± 0.2 μm non-CF, $P < 0.00005$). CBF was decreased in CF HBE monolayers (3.3 ± 0.2 Hz CF vs. 5.3 ± 0.3 Hz non-CF, $P < 0.0005$), potentially reflecting increased mucus viscosity, because abnormal ciliary beating is not believed to be primarily affected by the absence of CFTR function (33, 34). Although MCT was regionally variable among WT controls, CF monolayers uniformly exhibited minimal MCT (0.8 ± 0.4 mm/min CF vs. 10.4 ± 4.7 mm/min non-CF, $P < 0.05$).

Functional Anatomic Defects in CFTR (−/−) Piglet Trachea

Next, we addressed whether findings from HBE cultures were consistent with intact tissues that are more anatomically complex. We analyzed intact, full-thickness trachea explants from CFTR (−/−) piglets (hereinafter referred to as CF pigs) and CFTR (+/+) littermate control pigs (referred to as non-CF pigs) with μOCT under physiologic conditions (i.e., 37°C, 5% CO_2, and 100% humidity). The luminal surface of excised trachea was clearly visualized and demonstrated structural features of the anatomy including ASL, PCL, and both the epithelial layer and lamina propria (Figures 2A–2D and Video 2). Similar to cultured HBE cells, swine trachea showed a heterogeneous ASL and PCL across the epithelial surface that mirrored the anatomic variation of the mucosal folds. Nevertheless, compared with littermate control pigs, the ASL and PCL were reduced in CF trachea, and the cilia flattened. Submucosal glands were also evident by μOCT, enabling three-dimensional image reconstruction to evaluate the ductal lumen (Figures 2E and 2F). Within the glands, the non-CF pigs demonstrated evidence of a thin liquid layer surrounding the mucus being extruded, whereas this layer was absent in the CF trachea, akin to PCL depletion and indicative of reduced glandular output.

The above qualitative comparisons of CF and non-CF piglet airway microanatomy were confirmed using quantitative μOCT analysis (Figures 2G–2J and Video 2). The ASL depth of CF piglets was reduced compared with non-CF littermates (3.2 ± 0.8 μm CF vs. 9.2 ± 1.8 μm non-CF, $P < 0.05$). As observed in HBE monolayers, differences in the PCL depth were even more readily detected (3.2 ± 0.8 μm CF vs. 6.5 ± 0.2 μm non-CF, $P < 0.005$). The CBF of CF piglets was lower compared with control piglets (5.4 ± 0.9 Hz in CF vs. 10.6 ± 1.5 Hz in non-CF, $P < 0.05$). Although unstimulated MCT of non-CF piglet was brisk (1.8 ± 0.9 mm/min) and similar to measures of non-CF swine trachea made under physiologic conditions (24, 35, 36), CF MCT was severely delayed (0.2 ± 0.1 mm/min, $P < 0.05$).

The Effect of Shear Stress on Functional Microanatomy

Shear stress caused by breathing stimulates non-CFTR–dependent fluid secretion (37), and its absence in excised piglet tracheal samples may alter measured PCL depths. To control for this, we evaluated the effect of physiologically relevant shear on the functional microanatomy of excised trachea. Synchronous regional parameters were derived for each airway. Paired analyses of measurements are represented in Figure E2. Analogous to previous cell culture experiments (38), the PCL depth in both CF (6.1 ± 1.1 μm static vs. 7.9 ± 1.2 μm shear stress, $P < 0.00005$) and non-CF (8.6 ± 1.4 μm static vs. 10.4 ± 1.2 μm shear stress, $P < 0.0005$) trachea were augmented when exposed to shear stress for 4 hours before μOCT imaging (Figure 3A). Nevertheless, the PCL depth of CF trachea

was less than non-CF trachea, even when both tissues were under shear ($P < 0.0005$). Shear stress augmented CBF, but the effect was specific to CF piglet trachea (10.0 ± 1.2 Hz static vs. 13.8 ± 0.6 Hz shear stress, $P < 0.05$; Figure 3C). This result suggested that ciliary beating may be slowed in CF by abnormally viscous ASL, whereas normal ASL viscosity in non-CF tissues does not limit CBF. Changes in MCT with shear were not as sensitive to differences between conditions due to greater heterogeneity across the airway surface, but generally mirrored changes in PCL depth (Figure 3D). Additionally, the CF tracheae without shear stress had scant mucus particles present, making MCT comparisons more difficult. ASL depth increased with shear in non-CF tissues ($P < 0.005$; Figure 3B). Under shear, the CF ASL was less than non-CF ASL ($P < 0.005$), although the heterogeneity of this parameter could explain why the distinction between CF and non-CF ASL depths can be difficult to discern with less precise methods.

Relationships between the Airway Surface and Mucociliary Transport

Because the role of ASL depletion in CF pathogenesis remains a topic of considerable interest (1, 15, 39, 40), we sought to better understand the interrelationships between the various functional parameters of the airway surface, which were colocalized and simultaneously obtained using μOCT, a unique advantage of the assay. In non-CF piglet trachea, MCT rate was directly related to PCL depth (m = 0.93 ± 0.43, $P < 0.05$; Figure 4A), a phenomenon that has been frequently invoked but never before experimentally observed (1, 5, 6, 40), and reflects the importance of PCL hydration on maintaining MCC in the normal situation. The strong linear relationship between these parameters was also augmented by the application of shear stress, which was associated with the highest transport rates (Figure E3). In contrast, in CF trachea, the relationship between PCL depth and MCT was completely reversed, with greater PCL depths associated with the slowest transport rates (m = −0.52 ± 0.42, $P < 0.05$ vs. non-CF control; Figure 4B). When analysis was restricted to regions that exhibited adequate PCL hydration (≥7 μm), MCT was still reduced in CF (Figure 4C). Together, these

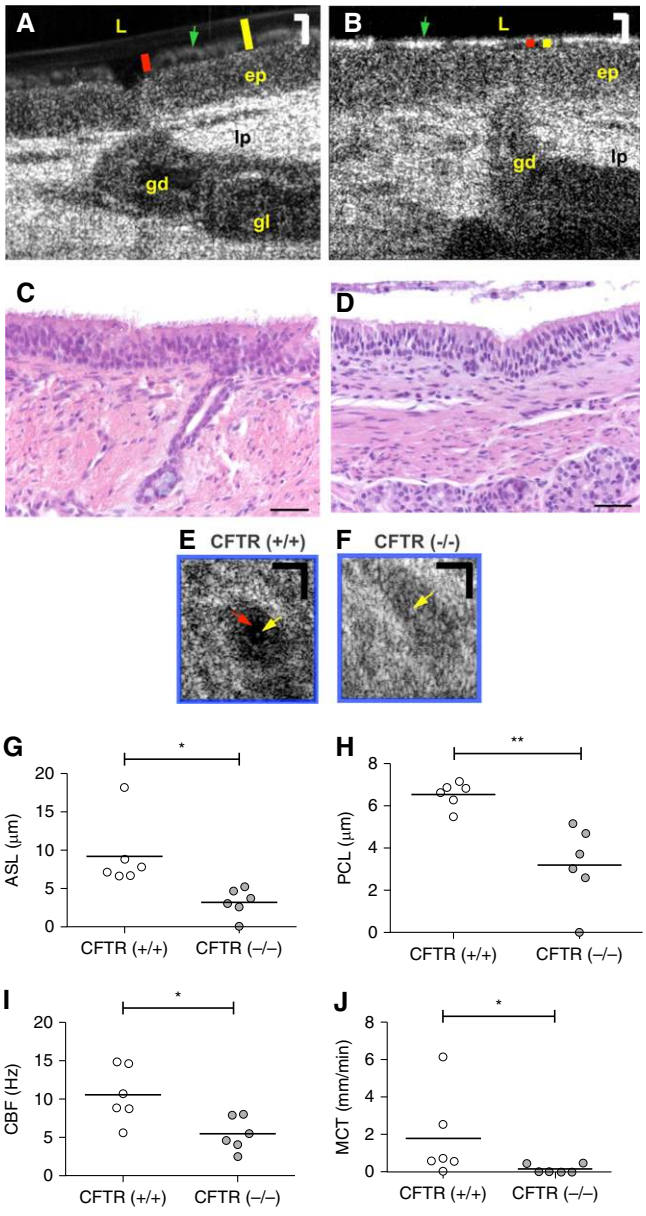

Figure 2. Microoptical coherence tomography (μOCT) imaging of swine trachea epithelia. (*A*) μOCT image of trachea explanted from a cystic fibrosis transmembrane conductance regulator (CFTR) (+/+) piglet clearly shows cilia tips (*green arrow*), airway surface liquid (ASL; *yellow bar*), and periciliary liquid (PCL; *red bar*) on the luminal surface (L). Epithelium (ep), lamina propria (lp), a gland (gl), and a gland duct (gd) transecting the image are also visualized. (*B*) Depleted ASL (*yellow bar*) and PCL (*red bar*) and flattened cilia (*green arrow*) are visible in a μOCT image of tracheal lumen (L) dissected from a CFTR (−/−) newborn piglet. Horizontal and vertical scale bars: 10 μm. (*C*, *D*) Histologic specimen stained with hematoxylin and eosin of corresponding area of CFTR (+/+) (*C*) and CFTR (−/−) (*D*) trachea. Scale bars: 34 μm. (*E*, *F*) Three-dimensional reconstructed *en face* view of representative duct glands from μOCT imaging. CFTR (+/+) piglet in *E* clearly shows a thin liquid layer (*red arrow*) surrounding the mucus within the gland duct (*yellow arrow*), which is not seen in the CFTR (−/−) piglet (*F*). Horizontal and vertical scale bars: 10 μm. *See* also Video 2. (*G*–*J*) Analysis of μOCT images from explanted swine yields numerical values for functional and anatomic parameters. ASL depth (*G*), PCL depth (*H*), ciliary beat frequency (CBF; *I*), and mucociliary transport (MCT) rate (*J*) are shown. **P* < 0.05, ***P* < 0.005. Each symbol represents mean value from independent trachea explant taken from five regions of interest. Note: A component of CFTR (+/+) control data was previously published in tabular format (10, 24).

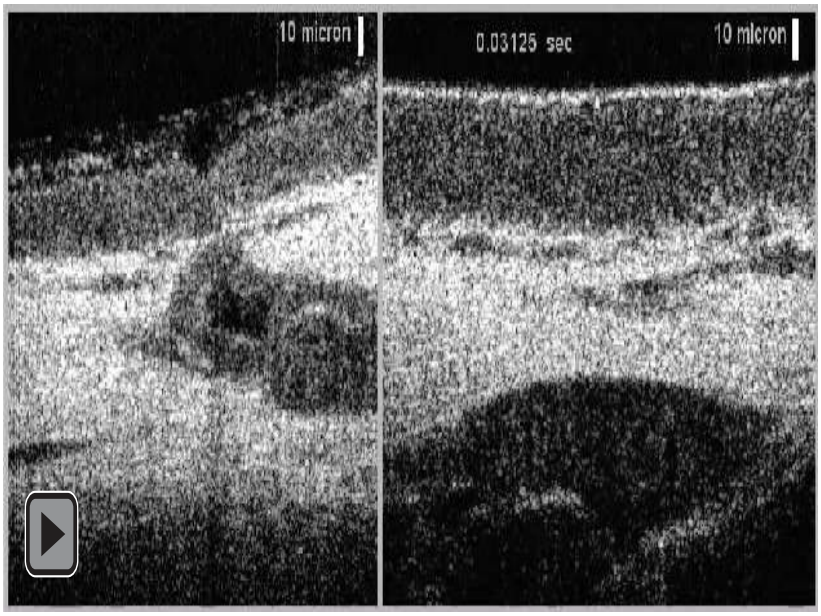

Video 2. Microoptical coherence tomography (μOCT) video showing intact, full-thickness swine trachea explants from a cystic fibrosis transmembrane conductance regulator (CFTR) (+/+) piglet (*left*) and a CFTR (−/−) piglet (*right*).

findings suggested a primary defect in the physical properties of airway mucus attributable to absent CFTR, which would be expected to disturb the normal relationship between adequate PCL hydration and intact MCT. Analysis of the correlation between ASL depth and MCT showed similar trends (Figures 4D and 4E). The aberrant PCL to MCT relationship in CF was not due to defective ciliary beating, because increased MCT was directly related to accelerated CBF in CF swine ($m = 0.33 \pm 0.18$, $P = 0.08$; Figure 4G). The association was not evident in non-CF trachea ($m = 0.09 \pm 0.21$, P = not significant for nonzero slope; Figure 4F), suggesting mucus viscosity is not limiting in this situation.

Studies of ASL viscosity *in situ* by fluorescence recovery after photobleaching indicated increased half-life of recovery in both CF piglet trachea (Figures 5A and 5B) and primary CF HBE cells (Figure 5C). These data confirmed that viscosity of the entire ASL layer was increased, complementing previous reports of increased ASL viscosity in excised human CF explants (8). Complementary studies evaluating the effective viscosity of the airway surface *in situ* using particle tracking microrheology in the absence of ciliary beating also identified elevated effective viscosity of the CF ASL (80.6 cP $\pm$ 26.5 CF vs. 12.0 $\pm$ 3.6 control, $P < 0.05$; Figures 5D–5F and Figure E4).

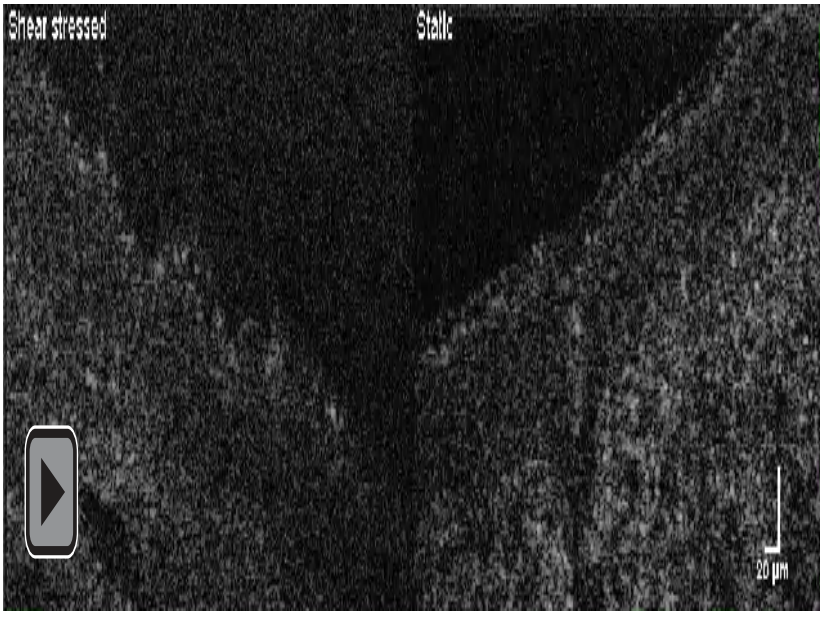

Video 3. Microoptical coherence tomography (μOCT) video showing intact, full-thickness swine trachea explants from a cystic fibrosis transmembrane conductance regulator (CFTR) (−/−) piglet exposed to shear stress (*left*) or control (*right*) conditions.

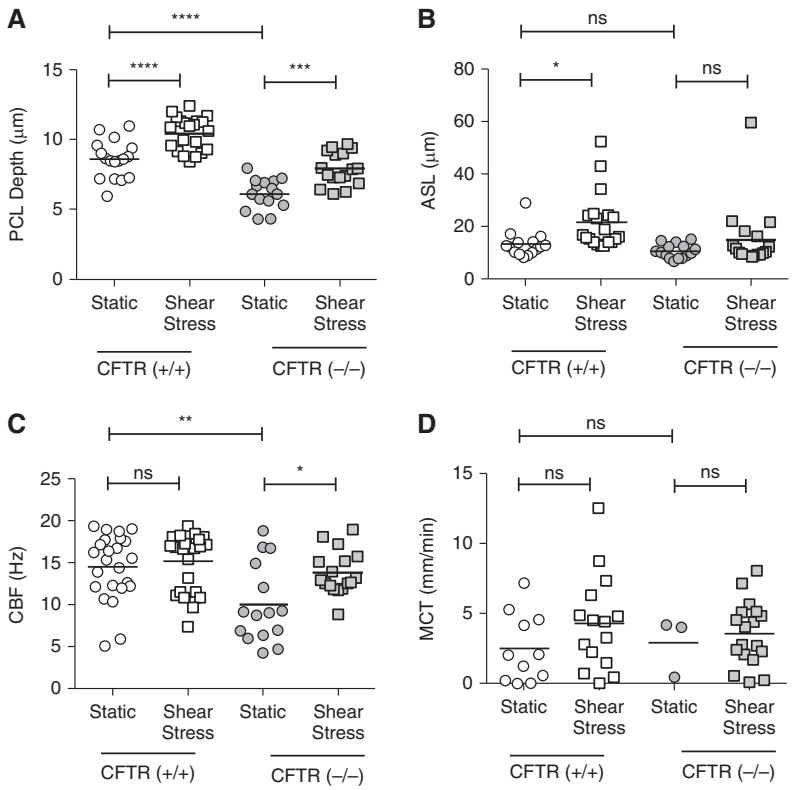

Figure 3. Functional parameters of swine tracheal epithelia with and without shear stress. Analysis of μOCT images from swine tracheal epithelia incubated under physiologic conditions and exposed to static environment or subjected to 0.114 dynes/cm^2 shear stress for 4 h before image acquisition. Periciliary liquid (PCL) depth (*A*), airway surface liquid depth (ASL, *B*), ciliary beat frequency (CBF, *C*), and mucociliary transport (MCT, *D*) are shown for each condition. Each symbol represents a single region of interest after static or shear stress exposure, as indicated. *$P < 0.05$, **$P < 0.005$, ***$P < 0.0005$, ****$P < 0.00005$. ns = not significant. *See* also Video 3.

Effect of Bicarbonate on Mucociliary Transport

Recent evidence suggests that bicarbonate may be important for normal mucus secretion and adherence in murine intestine (18, 19); hence, we hypothesized that blocking bicarbonate transport would adversely affect mucus transport even though it reflects only a small fraction of CFTR-mediated anion transport (2). Our findings focused on hydration within the PCL, because MCT and ciliary beating was most dependent on the status of this compartment and best reflected the influence of acute changes in fluid transport. As shown in representative time-averaged images (Figures 6A–6C), when normal adult pig trachea was treated with DNDS to inhibit bicarbonate transport (41), PCL depth was not significantly affected (7.1 ± 0.5 μm DNDS-treated vs. 7.8 ± 0.5 μm vehicle control, P = not significant; Figure 6D) but was reduced by bumetanide (6.4 ± 0.4 μm bumetanide-treated, $P < 0.05$; Figure 6D). Although PCL depth was undisturbed by treatment with DNDS, MCT was significantly reduced (1.1 ± 0.2 mm/min DNDS treated vs. 3.6 ± 0.7 mm/min vehicle control, $P < 0.05$; Figure 6E); bumetanide also reduced MCT (1.3 ± 0.6 mm/min, $P < 0.05$; Figure 6E). The relationship between PCL depth and MCT with DNDS treatment recapitulated the disrupted relationship observed in CF trachea (m = −0.19 ± 0.1, $P < 0.05$; Figure 6G), whereas bumetanide did not (m = −0.04 ± 0.4, P = not significant; Figure 6H). The effect of 4, 4-diisothiocyanatostilbene-2,2-disulfonic acid (DIDS), an alternative inhibitor of bicarbonate transport (42), was very similar (Figure E5). This suggested that the lack of bicarbonate is specifically responsible for the altered relationship between airway hydration and mucociliary transport in CF, likely secondary to altered physical properties of CF mucus. To confirm this, we conducted particle tracking microrheology on mucus collected from treated tracheae. Representative particle tracings are shown in Figure 6I, demonstrating that particle movement was more constrained in mucus collected from tracheae treated with DNDS (or bumetanide) compared with control. Also compared with control, both DNDS- and bumetanide-treated trachea secreted mucus with higher effective viscosity (Figure 6J, Figures E6A and E6B). To establish that bicarbonate transport was critical to these effects, normal HBE cells were cultured in bicarbonate-depleted media with and without the addition of acetazolamide, and particle tracking microrheology conducted on the mucus layer *in situ*. Particle displacement on the surface of cells grown in bicarbonate-depleted media were more constrained than particles on control cells (Figure 6K) and caused a significant increase in mucus viscosity, with or without addition of acetazolamide (Figure 6L, Figures E7A and E7B). Hence, bumetanide increased viscosity by dehydrating the PCL layer but did not alter the relationship between airway hydration and mucus transport. In contrast, lack of bicarbonate transport increased mucus viscosity and disrupted MCT without changing the PCL volume.

Discussion

Using μOCT, we established a relationship between PCL hydration and MCT rate that has been frequently hypothesized but never before been proven to operate in normal lung. By analyzing colocalized, synchronous measures of the airway functional anatomy, our findings further indicate that the MCT apparatus of the CF airway, and the impact of PCL hydration toward regulating mucus transport, are profoundly disrupted. Additional experimentation using FRAP and particle tracking reveal an abnormally viscous ASL, even in the absence of airway infection, which accounts for the abnormal relationship between PCL and MCT. In the CF airway, elevated mucus viscosity disturbs normal MCT by a mechanism that is independent of ciliary hydration and function. By selectively inhibiting either bicarbonate or chloride transport, we determined that bicarbonate regulates this abnormal relationship, even in the presence of adequate PCL hydration, and its absence recapitulates abnormal mucus viscosity and

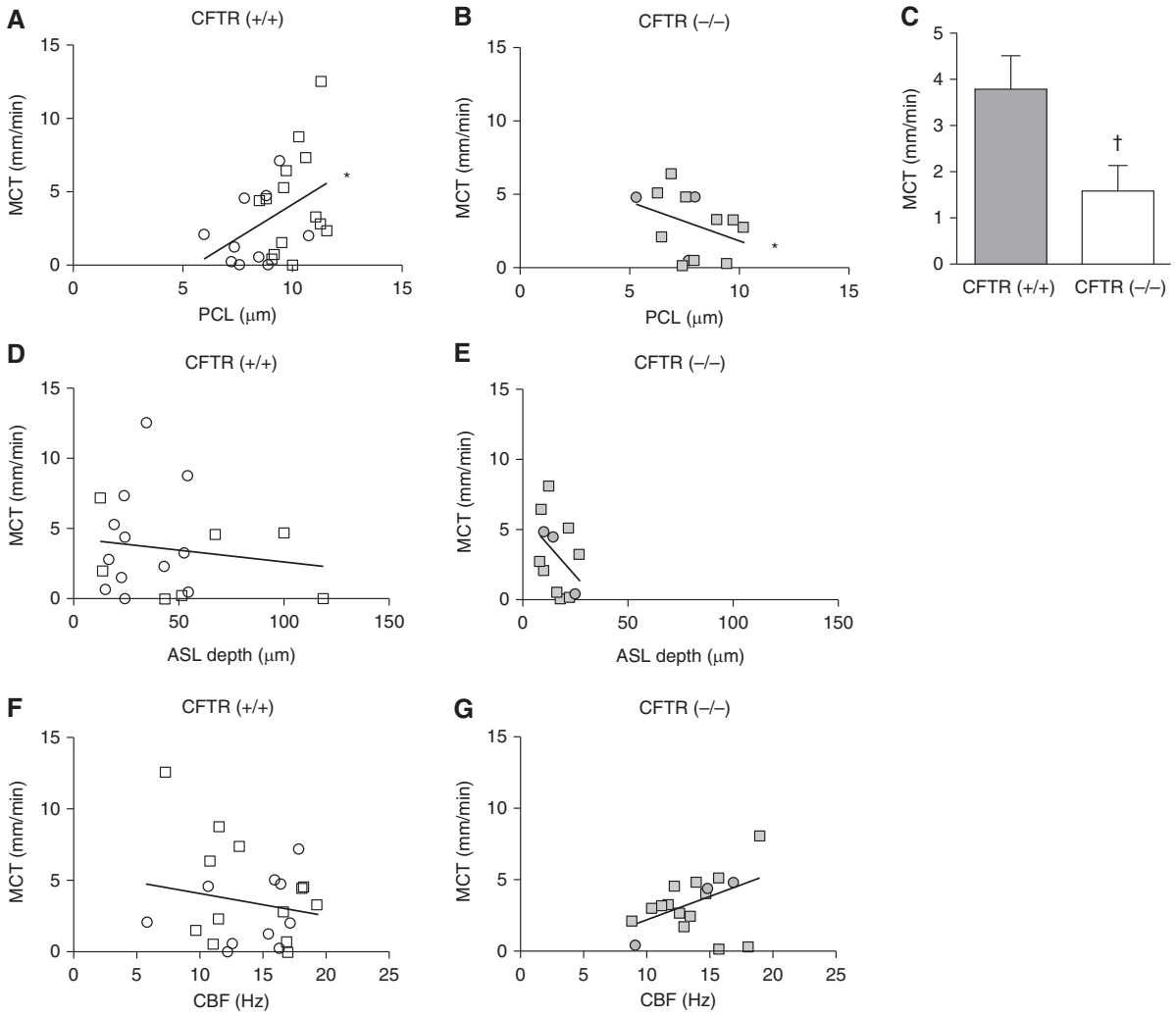

Figure 4. Altered functional microanatomy in cystic fibrosis (CF) swine trachea. (*A*, *B*) Correlation between periciliary liquid (PCL) and mucociliary transport (MCT) for CF transmembrane conductance regulator (CFTR) (+/+) trachea (*A*) and CFTR (−/−) trachea (*B*). Matched data from experiments after shear stress (*circles*) and static (*squares*) conditions are included. Linear curve fit in wild type (R^2 = 0.17, *$P < 0.05$) was significantly different than CF (R^2 = 0.12; *$P < 0.05$ for CF vs. non-CF slope comparison; P = 0.06 for linear fit). (*C*) MCT of CFTR (+/+) trachea compared with CFTR (−/−) trachea when PCL depth was ⩾7 μM. †P = 0.06. (*D*, *E*) Correlation between airway surface liquid (ASL) depth and MCT in CFTR (+/+) trachea (*D*) and CFTR (−/−) trachea (*E*). Linear curve fits for CFTR (+/+) (R^2 = 0.02, P = not significant) and CFTR (−/−) (R^2 = 0.21, P = 0.13) are shown. (*F*, *G*) Correlation between ciliary beat frequency (CBF) and MCT for CFTR (+/+) trachea (*F*) and CFTR (−/−) trachea (*G*). Linear curve fit for CFTR (+/+) (R^2 = 0.03, P = not significant) and CFTR (−/−) (R^2 = 0.18, P = 0.08) are shown.

mucociliary transport evident in the CF airway. Because these studies were performed in fresh tissues of newborn piglet and sterile human airway cultures, the results reflect the underlying mechanisms of CF rather than secondary phenomena such as infection or inflammation that can occur in the infected lung. These findings are significant, because they show that mucoviscidosis, in addition to relative PCL depletion, is operative in the CF airway and prominently contributes to delayed MCT in the disease (21).

This study reveals an interrelationship between PCL depth and MCT rates on a regional basis, based on the analysis of colocalized and simultaneous measurements of the functional microanatomy. These results validate a longstanding hypothesis that PCL hydration is an essential contributor to the maintenance of normal MCT (1, 8, 39, 40, 43) and provide a basis for understanding how "hydration therapies," such as hypertonic saline (44, 45), mannitol (46), or ENaC inhibitors (47), augment airway defense. However, given that increased native PCL depth was not associated with accelerated MCT in CF epithelia, the results also indicate that PCL depletion is not the sole contributor to mucus stasis in the CF airway. Although the biochemical origin of increased mucus viscosity in CF has not been proven, abnormal mucin expansion and adhesion due to molecular events that require intact CFTR-mediated bicarbonate secretion have recently been proposed as features of the CF defect that could result in increased effective viscosity (18, 19, 48). Intact bicarbonate transport was crucial to maintaining acetylcholine-stimulated MCT in excised swine trachea, leading Cooper and colleagues to speculate that viscosity could be a contributing factor

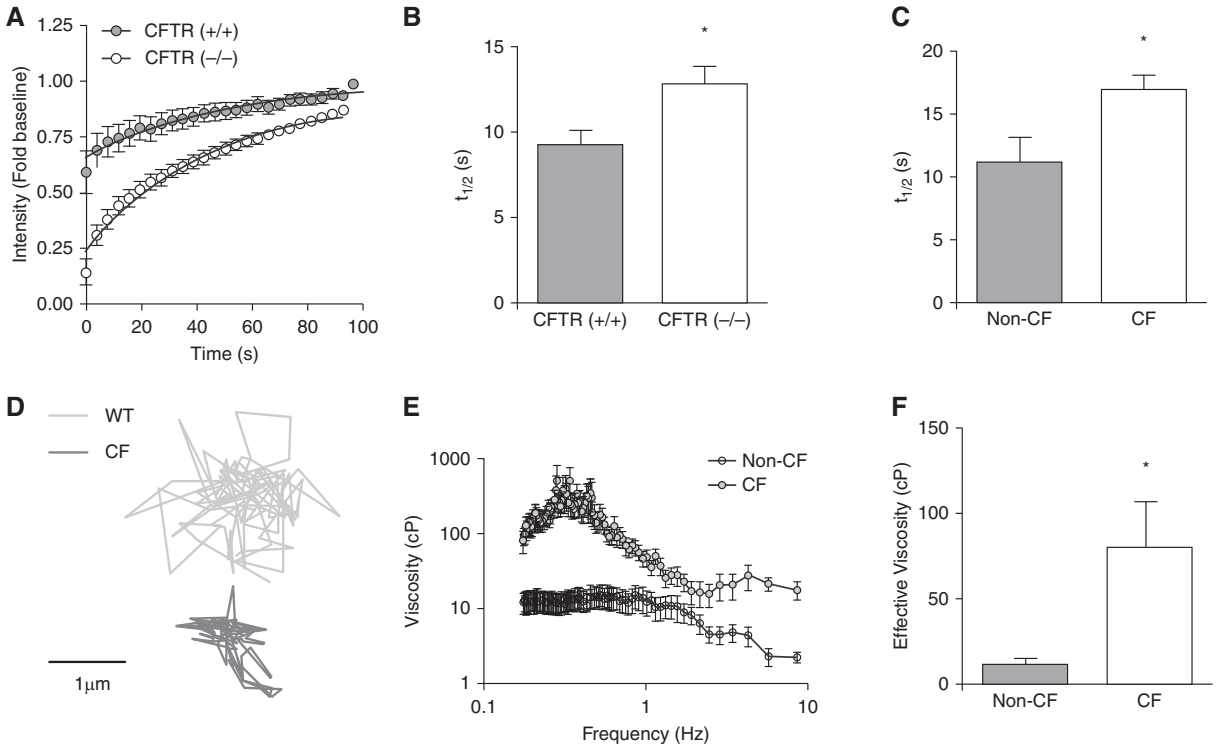

Figure 5. Mucus viscosity *in situ*. (*A–C*) Viscosity of airway surface liquid detected by fluorescence recovery after photobleaching (FRAP). (*A*) Representative FRAP curve of airway mucus *in situ* from cystic fibrosis transmembrane conductance regulator (CFTR) (+/+) and CFTR (−/−) piglets. (*B*, *C*) Summary data of FRAP half-life as determined in swine trachea explants (*B*) and primary human bronchial epithelial monolayers from derived from donors with cystic fibrosis (CF) and those without (non-CF) (*C*). *$P < 0.05$, n = 3–5 per condition. (*D*, *E*) Particle tracking microrheology of the airway surface liquid depth (ASL) of CF and non-CF airway monolayers after cessation of ciliary motion using 0.1% benzalkonium chloride. (*D*) Representative 2.2-s particle track of 50-nm polyethylene glycol–coated particle in the ASL of CF and non-CF airway monolayers. Scale bar = 1 μm. (*E*) Frequency-dependent dynamic viscosity estimated from particle tracking. (*F*) Comparison of the viscosities obtained at the lowest frequency assessed (0.175 Hz) represents effective viscosity of CF and non-CF monolayers. $P < 0.05$, n = 12 per condition.

(36), findings also reported by Jayaraman and colleagues in excised tissues using FRAP (49). Our findings are consistent with these studies and implicate an inherent abnormality of CF mucus that is dependent on bicarbonate transport. Along with newly recognized defects in microbial killing due to acidic pH (16, 17) and abnormal mucus adhesion observed in the intestine of murine CF models that may also be dependent on adequate CFTR-dependent bicarbonate transport (18, 19), the failure to maintain normal MCT despite adequate PCL depth represents a fundamental characteristic of the CF airway and could impact airway defense (50). Notably, these conclusions could account for the disproportionate severity of lung disease in CF when compared with other disorders of MCC such as primary ciliary dyskinesia, which results in complete abrogation of the MCT apparatus but is not impacted by innate CFTR-dependent defects of the mucus itself (51).

Under static, steady-state conditions, we observed many features traditionally ascribed to CF pulmonary pathogenesis, including reduced PCL and ASL depth (6, 52, 53), diminished CBF (34), and delayed MCT rates (6). These findings were consistent and observed in both cultured HBE cells *in vitro* and living *ex vivo* piglet trachea. Our findings in cell culture were in agreement with studies by several laboratories using a variety of traditional imaging techniques, providing additional confidence in the results (5, 6, 9, 27, 38, 53). In contrast, the studies in piglet tissues conflicted with a recent report that did not demonstrate decreased PCL depth in 1-day-old CF piglets when studied by OsO_4 fixation (15). Because μOCT can measure the PCL depth by visualizing the fully extended length of the cilia without experimental manipulations, the technique may be more sensitive to differences than OsO_4 fixation and also incorporates the mucus layer, a parameter that is clearly more variable across anatomic regions. By demonstrating that the difference in PCL depth between WT and CF piglet trachea persists despite application of shear stress (Figure 3A), whereas the difference in ASL was less precise (Figure 3D), our studies offer a potential explanation for conflicting results and provide direct evidence that relative PCL depletion in CF occurs under physiologic conditions. Given the regional variation in PCL and ASL depths, ciliary beating, and MCT rates, it is likely that specific regions of the CF airway, such as the smallest airways or branch points, may be particularly susceptible to PCL depletion and subsequent mucus stasis due to defective airway hydration, even in the setting of normal breathing.

Although CF pigs have closely resembled human CF lung disease (13, 14, 54, 55), studies of human subjects are needed to address potential differences in the human condition, such as the effect of partially active CFTR alleles. Development

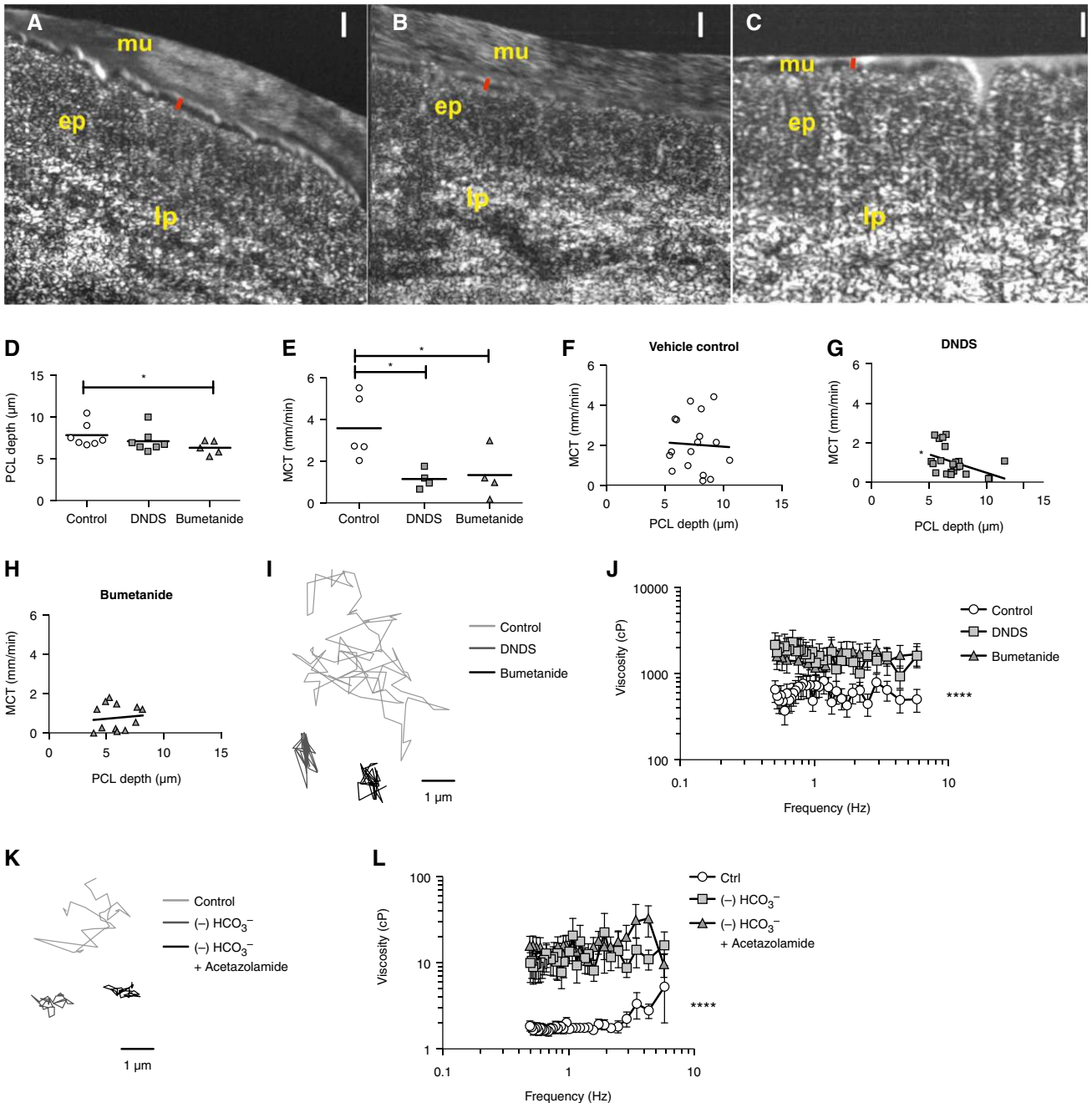

Figure 6. Inhibition of bicarbonate transport. (*A–C*) Representative time-averaged microoptical coherence tomography (μOCT) images of normal adult swine trachea treated with vehicle control (*A*), 4,4'-dinitrostilbene-2,2'-disulphonic acid (DNDS) (*B*), and bumetanide (*C*) clearly shows periciliary liquid (PCL; *red bar*) on the luminal surface. Epithelium (ep) and lamina propria (lp) are also visualized. Streaks above the PCL indicate a moving mucus layer (μ) in the vehicle- and DNDS-treated tracheae, whereas bumetanide-treated trachea indicate a scant mucus layer except near a gland. Scale (*white bar*) = 10 μm. (*D*) Quantification of PCL depth shows no effect of DNDS treatment on this compartment, whereas PCL depths are reduced in tissue treated with bumetanide. (*E*). Measurement of mucociliary transport (MCT) rate showed reduced transport in tissues treated with both DNDS and bumetanide. (*F–H*) Linear curve fits for a relationship between PCL depth and MCT rate in vehicle control (*F*; R^2 = 0.007, *P* = not significant), DNDS-treated (*G*; R^2 = 0.178, *P* = 0.04), and bumetanide-treated (*H*; R^2 = 0.001, *P* = not significant) are shown. (*I*) Particle tracking microrheology of the mucus collected from these trachea yielded 2.2-s representative particle tracks of 500-nm polyethylene glycol–coated particle in the mucus of vehicle control–, DNDS-, and bumetanide-treated tissues. Scale bar = 1 μm. (*J*) Frequency-dependent dynamic viscosity curves of these mucus samples show significantly higher viscosities in mucus from both DNDS and bumetanide-treated tracheae compared with control. (*K*) Particle-tracking microrheology of the mucus layer of normal airway monolayers cultured in normal media and bicarbonate-depleted media with and without acetazolamide yields representative particle tracks of 500-nm polyethylene glycol–coated particle. Scale bar = 1 μm. (*L*) Frequency-dependent dynamic viscosity curves of these mucus samples show significantly higher viscosities in mucus on cells incubated in bicarbonate-depleted media, both with and without acetazolamide, compared with control. *$P < 0.05$, ****$P < 0.0001$.

of colocalized measures of mucus viscosity within various layers of the ASL could also provide additional information as to the origin of the defect and could be possible with native particle tracking in the future. ■

Author disclosures are available with the text of this article at www.atsjournals.org.

Acknowledgment: The authors thank Arianne Fulce, Kathy Sexton, Thurman Richardson, and the Tissue Collection and Banking Facility at University of Alabama at Birmingham (UAB) for services related to airway tissue procurement. They also thank Joan Cadillac for veterinary assistance with the adult pigs. The authors thank Heather Hathorne for regulatory support for work with human subjects and the patients who donated their organs for these experiments. The authors acknowledge assistance from the UAB Imaging Core Facility and Prof. Mei Wu's laboratory in the Wellman Center of Photomedicine, Massachusetts General Hospital (MGH). Piglet airway tissue was obtained from Exemplar Genetics Inc.; adult pigs were obtained from Auburn University and the MGH Knight Surgical Laboratory.

References

1. Rowe SM, Miller S, Sorscher EJ. Cystic fibrosis. *N Engl J Med* 2005;352: 1992–2001.
2. Poulsen JH, Fischer H, Illek B, Machen TE. Bicarbonate conductance and pH regulatory capability of cystic fibrosis transmembrane conductance regulator. *Proc Natl Acad Sci USA* 1994;91:5340–5344.
3. Quinton PM. Missing Cl conductance in cystic fibrosis. *Am J Physiol* 1986;251:C649–C652.
4. Welsh MJ. An apical-membrane chloride channel in human tracheal epithelium. *Science* 1986;232:1648–1650.
5. Matsui H, Randell SH, Peretti SW, Davis CW, Boucher RC. Coordinated clearance of periciliary liquid and mucus from airway surfaces. *J Clin Invest* 1998;102:1125–1131.
6. Matsui H, Grubb BR, Tarran R, Randell SH, Gatzy JT, Davis CW, Boucher RC. Evidence for periciliary liquid layer depletion, not abnormal ion composition, in the pathogenesis of cystic fibrosis airways disease. *Cell* 1998;95:1005–1015.
7. Tarran R. Regulation of airway surface liquid volume and mucus transport by active ion transport. *Proc Am Thorac Soc* 2004;1:42–46.
8. Song Y, Namkung W, Nielson DW, Lee JW, Finkbeiner WE, Verkman AS. Airway surface liquid depth measured in ex vivo fragments of pig and human trachea: dependence on Na+ and Cl- channel function. *Am J Physiol Lung Cell Mol Physiol* 2009;297:L1131–L1140.
9. Van Goor F, Hadida S, Grootenhuis PD, Burton B, Cao D, Neuberger T, Turnbull A, Singh A, Joubran J, Hazlewood A, *et al*. Rescue of CF airway epithelial cell function in vitro by a CFTR potentiator, VX-770. *Proc Natl Acad Sci USA* 2009;106:18825–18830.
10. Joo NS, Saenz Y, Krouse ME, Wine JJ. Mucus secretion from single submucosal glands of pig. Stimulation by carbachol and vasoactive intestinal peptide. *J Biol Chem* 2002;277:28167–28175.
11. Joo NS, Irokawa T, Wu JV, Robbins RC, Whyte RI, Wine JJ. Absent secretion to vasoactive intestinal peptide in cystic fibrosis airway glands. *J Biol Chem* 2002;277:50710–50715.
12. Jayaraman S, Joo NS, Reitz B, Wine JJ, Verkman AS. Submucosal gland secretions in airways from cystic fibrosis patients have normal [Na(+)] and pH but elevated viscosity. *Proc Natl Acad Sci USA* 2001; 98:8119–8123.
13. Stoltz DA, Meyerholz DK, Pezzulo AA, Ramachandran S, Rogan MP, Davis GJ, Hanfland RA, Wohlford-Lenane C, Dohrn CL, Bartlett JA, *et al*. Cystic fibrosis pigs develop lung disease and exhibit defective bacterial eradication at birth. *Sci Transl Med* 2010;2:29ra31.
14. Rogers CS, Stoltz DA, Meyerholz DK, Ostedgaard LS, Rokhlina T, Taft PJ, Rogan MP, Pezzulo AA, Karp PH, Itani OA, *et al*. Disruption of the CFTR gene produces a model of cystic fibrosis in newborn pigs. *Science* 2008;321:1837–1841.
15. Chen JH, Stoltz DA, Karp PH, Ernst SE, Pezzulo AA, Moninger TO, Rector MV, Reznikov LR, Launspach JL, Chaloner K, *et al*. Loss of anion transport without increased sodium absorption characterizes newborn porcine cystic fibrosis airway epithelia. *Cell* 2010;143: 911–923.
16. Pezzulo AA, Tang XX, Hoegger MJ, Alaiwa MH, Ramachandran S, Moninger TO, Karp PH, Wohlford-Lenane CL, Haagsman HP, van Eijk M, *et al*. Reduced airway surface pH impairs bacterial killing in the porcine cystic fibrosis lung. *Nature* 2012;487:109–113.
17. Abou Alaiwa MH, Beer AM, Pezzulo AA, Launspach JL, Horan RA, Stoltz DA, Starner TD, Welsh MJ, Zabner J. Neonates with cystic fibrosis have a reduced nasal liquid pH; a small pilot study. *J Cyst Fibros* 2014;13:373–377.
18. Garcia MA, Yang N, Quinton PM. Normal mouse intestinal mucus release requires cystic fibrosis transmembrane regulator-dependent bicarbonate secretion. *J Clin Invest* 2009;119:2613–2622.
19. Gustafsson JK, Ermund A, Ambort D, Johansson ME, Nilsson HE, Thorell K, Hebert H, Sjövall H, Hansson GC. Bicarbonate and functional CFTR channel are required for proper mucin secretion and link cystic fibrosis with its mucus phenotype. *J Exp Med* 2012; 209:1263–1272.
20. Derichs N, Jin BJ, Song Y, Finkbeiner WE, Verkman AS. Hyperviscous airway periciliary and mucous liquid layers in cystic fibrosis measured by confocal fluorescence photobleaching. *FASEB J* 2011; 25:2325–2332.
21. Quinton PM. Cystic fibrosis: impaired bicarbonate secretion and mucoviscidosis. *Lancet* 2008;372:415–417.
22. Shamsuddin AK, Quinton PM. Native small airways secrete bicarbonate. *Am J Respir Cell Mol Biol* 2014;50:796–804.
23. Bush A, Payne D, Pike S, Jenkins G, Henke MO, Rubin BK. Mucus properties in children with primary ciliary dyskinesia: comparison with cystic fibrosis. *Chest* 2006;129:118–123.
24. Liu L, Chu KK, Houser GH, Diephuis BJ, Li Y, Wilsterman EJ, Shastry S, Dierksen G, Birket SE, Mazur M, *et al*. Method for quantitative study of airway functional microanatomy using micro-optical coherence tomography. *PLoS ONE* 2013;8:e54473.
25. Liu L, Gardecki JA, Nadkarni SK, Toussaint JD, Yagi Y, Bouma BE, Tearney GJ. Imaging the subcellular structure of human coronary atherosclerosis using micro-optical coherence tomography. *Nat Med* 2011;17:1010–1014.
26. Tuggle KL, Birket SE, Cui X, Hong J, Warren J, Reid L, Chambers A, Ji D, Gamber K, Chu KK, *et al*. Characterization of defects in ion transport and tissue development in cystic fibrosis transmembrane conductance regulator (CFTR)-knockout rats. *PLoS ONE* 2014;9: e91253.
27. Sloane PA, Shastry S, Wilhelm A, Courville C, Tang LP, Backer K, Levin E, Raju SV, Li Y, Mazur M, *et al*. A pharmacologic approach to acquired cystic fibrosis transmembrane conductance regulator dysfunction in smoking related lung disease. *PLoS ONE* 2012;7: e39809.
28. Raju SV, Jackson PL, Courville CA, McNicholas CM, Sloane PA, Sabbatini G, Tidwell S, Tang LP, Liu B, Fortenberry JA, *et al*. Cigarette smoke induces systemic defects in cystic fibrosis transmembrane conductance regulator function. *Am J Respir Crit Care Med* 2013;188:1321–1330.
29. Neuberger T, Burton B, Clark H, Van Goor F. Use of primary cultures of human bronchial epithelial cells isolated from cystic fibrosis patients for the pre-clinical testing of CFTR modulators. *Methods Mol Biol* 2011;741:39–54.
30. Ballard ST, Trout L, Bebök Z, Sorscher EJ, Crews A. CFTR involvement in chloride, bicarbonate, and liquid secretion by airway submucosal glands. *Am J Physiol* 1999;277:L694–L699.
31. Mason TG, Ganesan K, van Zanten JH, Wirtz D, Kuo SC. Particle tracking microrheology of complex fluids. *Phys Rev Lett* 1997;79: 3282.
32. Suh J, Dawson M, Hanes J. Real-time multiple-particle tracking: applications to drug and gene delivery. *Adv Drug Deliv Rev* 2005;57: 63–78.
33. Rutland J, Cole PJ. Nasal mucociliary clearance and ciliary beat frequency in cystic fibrosis compared with sinusitis and bronchiectasis. *Thorax* 1981;36:654–658.

34. Schmid A, Sutto Z, Schmid N, Novak L, Ivonnet P, Horvath G, Conner G, Fregien N, Salathe M. Decreased soluble adenylyl cyclase activity in cystic fibrosis is related to defective apical bicarbonate exchange and affects ciliary beat frequency regulation. *J Biol Chem* 2010;285:29998–30007.
35. Ballard ST, Trout L, Mehta A, Inglis SK. Liquid secretion inhibitors reduce mucociliary transport in glandular airways. *Am J Physiol Lung Cell Mol Physiol* 2002;283:L329–L335.
36. Cooper JL, Quinton PM, Ballard ST. Mucociliary transport in porcine trachea: differential effects of inhibiting chloride and bicarbonate secretion. *Am J Physiol Lung Cell Mol Physiol* 2013; 304:L184–L190.
37. Tarran R, Button B, Boucher RC. Regulation of normal and cystic fibrosis airway surface liquid volume by phasic shear stress. *Annu Rev Physiol* 2006;68:543–561.
38. Tarran R, Button B, Picher M, Paradiso AM, Ribeiro CM, Lazarowski ER, Zhang L, Collins PL, Pickles RJ, Fredberg JJ, *et al*. Normal and cystic fibrosis airway surface liquid homeostasis. The effects of phasic shear stress and viral infections. *J Biol Chem* 2005;280: 35751–35759.
39. Itani OA, Chen JH, Karp PH, Ernst S, Keshavjee S, Parekh K, Klesney-Tait J, Zabner J, Welsh MJ. Human cystic fibrosis airway epithelia have reduced Cl- conductance but not increased Na+ conductance. *Proc Natl Acad Sci USA* 2011;108:10260–10265.
40. Guggino WB. Cystic fibrosis salt/fluid controversy: in the thick of it. *Nat Med* 2001;7:888–889.
41. Shan J, Huang J, Liao J, Robert R, Hanrahan JW. Anion secretion by a model epithelium: more lessons from Calu-3. *Acta Physiol (Oxf)* 2011;202:523–531.
42. Inglis SK, Corboz MR, Taylor AE, Ballard ST. Effect of anion transport inhibition on mucus secretion by airway submucosal glands. *Am J Physiol* 1997;272:L372–L377.
43. Boucher RC. Human airway ion transport. Part two. *Am J Respir Crit Care Med* 1994;150:581–593.
44. Elkins MR, Robinson M, Rose BR, Harbour C, Moriarty CP, Marks GB, Belousova EG, Xuan W, Bye PT; National Hypertonic Saline in Cystic Fibrosis (NHSCF) Study Group. A controlled trial of long-term inhaled hypertonic saline in patients with cystic fibrosis. *N Engl J Med* 2006;354:229–240.
45. Donaldson SH, Bennett WD, Zeman KL, Knowles MR, Tarran R, Boucher RC. Mucus clearance and lung function in cystic fibrosis with hypertonic saline. *N Engl J Med* 2006;354:241–250.
46. Aitken ML, Bellon G, De Boeck K, Flume PA, Fox HG, Geller DE, Haarman EG, Hebestreit HU, Lapey A, Schou IM, *et al*.; CF302 Investigators. Long-term inhaled dry powder mannitol in cystic fibrosis: an international randomized study. *Am J Respir Crit Care Med* 2012;185:645–652.
47. Mall MA. Role of the amiloride-sensitive epithelial Na+ channel in the pathogenesis and as a therapeutic target for cystic fibrosis lung disease. *Exp Physiol* 2009;94:171–174.
48. Quinton PM. Role of epithelial $HCO3^-$ transport in mucin secretion: lessons from cystic fibrosis. *Am J Physiol Cell Physiol* 2010;299: C1222–C1233.
49. Jayaraman S, Song Y, Vetrivel L, Shankar L, Verkman AS. Noninvasive in vivo fluorescence measurement of airway-surface liquid depth, salt concentration, and pH. *J Clin Invest* 2001;107:317–324.
50. Schneider WR, Doetsch RN. Effect of viscosity on bacterial motility. *J Bacteriol* 1974;117:696–701.
51. Cohen-Cymberknoh M, Yaakov Y, Shoseyov D, Shteyer E, Schachar E, Rivlin J, Bentur L, Picard E, Aviram M, Israeli E, *et al*. Evaluation of the intestinal current measurement method as a diagnostic test for cystic fibrosis. *Pediatr Pulmonol* 2013;48:229–235.
52. Zhang L, Button B, Gabriel SE, Burkett S, Yan Y, Skiadopoulos MH, Dang YL, Vogel LN, McKay T, Mengos A, *et al*. CFTR delivery to 25% of surface epithelial cells restores normal rates of mucus transport to human cystic fibrosis airway epithelium. *PLoS Biol* 2009;7: e1000155.
53. Harvey PR, Tarran R, Garoff S, Myerburg MM. Measurement of the airway surface liquid volume with simple light refraction microscopy. *Am J Respir Cell Mol Biol* 2011;45:592–599.
54. Stoltz DA, Rokhlina T, Ernst SE, Pezzulo AA, Ostedgaard LS, Karp PH, Samuel MS, Reznikov LR, Rector MV, Gansemer ND, *et al*. Intestinal CFTR expression alleviates meconium ileus in cystic fibrosis pigs. *J Clin Invest* 2013;123:2685–2693.
55. Ostedgaard LS, Meyerholz DK, Chen JH, Pezzulo AA, Karp PH, Rokhlina T, Ernst SE, Hanfland RA, Reznikov LR, Ludwig PS, *et al*. The ΔF508 mutation causes CFTR misprocessing and cystic fibrosis-like disease in pigs. *Sci Transl Med* 2011;3:74ra24.